Multiple Reduced Order Models for Antenna Measurements

Samuel Corre, Laurent Le Coq, Benjamin Fuchs, Michael Mattes, Nicolas Mézières

Multiple Reduced Order Models for Antenna Measurements

Samuel Corre*, Laurent Le Coq*, Benjamin Fuchs†, Michael Mattes‡, Nicolas Mézières§
*IETR, Université de Rennes, Rennes, France
† Federal Office of Communications, Biel, Switzerland
‡ DTU Space, Technical University of Denmark, Denmark
§ CNES, Toulouse, France

***Abstract*—For the characterization of the radiated field of antennas, the Reduced Order Model method is a simple yet powerful numerical tool that allows to reduce significantly the number of field samples relatively to other techniques based on analytical signal expansions. To further improve the flexibility and versatility of this tool, this article focuses on building a set of multiple reduced models via subdivision of the source domain and on applying reference point method for ROM. Validations based on simulation and measurement data in the far field are shown.**

***Index Terms*—Antenna measurements, antenna radiation pattern, reduced order systems.**

I. Introduction

The characterization of the radiated field of antennas is mathematically an expansion of a sampled/measured signal in some function basis. This basis allows the interpolation of the field between the sampling positions on the measurement surface or a complete 3D reconstruction. The standard approaches rely on analytical functions such as Spherical Waves [1] or Plane Waves [2] for which convenient and powerful sampling theorems exist. However, in the hope of further reducing the measurement constraints, techniques such as optimization algorithms or numerical models are appealing. They allow the introduction of additional knowledge to, for example, reduce the number of measurements samples. We may cite sparse recovery [3], exploiting the sparsity of field expansions on Spherical Waves, or even basis constructed by simulations of the system to be characterized [4]. In particular, a function basis can be deduced from the geometry of the antenna using the equivalent surface principle and a Reduced Order Model (ROM) approach [5], [6]. The idea of taking more geometrical information into account was already proposed years ago in [7] but in an analytical manner, imposing strong constraints on the possible geometries. While losing the mathematical certainty brought by analytical methods, the numerical basis obtained from ROM allows for more flexibility and is intrinsically tailored to both the Antenna Under Test (AUT) and measurement surface. To continue in that direction, in this article we propose a method, where multiple Reduced Order Models are coupled to form our antenna characterization problem. Although the approach is general and could be applied to both near and far field with no restriction on the field sampling surface, the presented studies have been carried out on the far field with a planar equivalent surface.

The article is organized as follows: in Section II, the ROM approach is quickly recalled and the multi-ROM method is presented along with some basic and useful properties. In Section III, the multi-ROM method is applied to simulated and measured data. Finally, conclusions are drawn in Section IV.

II. Multiresolution Strategy

A. Reduced Order Model

The equivalent surface principle [8] allows to represent any set of electromagnetic sources, in terms of radiated field, contained in a given surface Σ by equivalent (tangential) currents over Σ. By meshing the equivalent surface Σ and defining observation positions, one is able to discretize the radiation operator (between the equivalent currents and the field at the observations positions) into a radiation matrix $\mathbf{A}$. Once this matrix is computed, the ROM is obtained from $\mathbf{A}$ by performing its Singular Value Decomposition (SVD). The truncation of this SVD to the expected accuracy level leads to the so-called ROM. Extended details on this method can be found in [9] and [10]. If Σ is set around the AUT and the observation positions contain the measurement sampling on the measurement surface S, the characterization of the radiated field $\mathbf{y}$ is reduced to the resolution of a linear system

$$\mathbf{y} = \mathbf{U}\nu, \tag{1}$$

where $\mathbf{U}$ contains the said ROM, the tailored numerical basis and $\boldsymbol{\nu}$ is the unknown vector. This method has been proven to reduce significantly the number of field samples relatively to conventional approaches or even sparse recovery methods. It is therefore of interest to study in depth the properties and operations that one can perform on the basis produced by the ROM.

B. Surface Subdivision

1) Definition: Normally, a single ROM on the complete equivalent surface is computed. However, using multiple ROMs for a single problem is appealing to provide a more versatile tool, for example with adaptive orders depending on the region of Σ, that could be of interest for embedded antennas. In this article, a multi-ROM approach is proposed

by dividing the equivalent surface Σ into K subdomains Σ_k, with $k = 0, \ldots, K-1$ and $\cup_k \Sigma_k = \Sigma$. Thus, every subdomain Σ_k possesses its own radiation submatrix $\mathbf{A}_k$, and (up to a column permutation) $\mathbf{A} = \left[\mathbf{A}_0 \ldots \mathbf{A}_{K-1}\right]$. This division can be coupled with the ROM approach by doing:

$$\mathbf{y} = \tilde{\mathbf{U}}\tilde{\nu}, \tag{2}$$

where $\tilde{\mathbf{U}} = \left[\mathbf{U}_0 \ldots \mathbf{U}_{K-1}\right]$ and each $\mathbf{U}_k$ is obtained from the SVD of $\mathbf{A}_k$.

2) Truncation Order: The main interest of the ROM is to reduce the number of unknowns to be identified, represented by the size of ν in (1), in order to characterize the radiation pattern of the AUT. This number of unknowns is determined by the truncation order T of the SVD of the radiation matrix, which is obtained by the index at which the normalized singular value distribution of $\mathbf{A}$ crosses the expected level of accuracy. In the multi-ROM approach, a SVD is rather performed on each submatrix $\mathbf{A}_k$, where each one possesses its own truncation order T_k. Hence, the number of unknowns in the multi-ROM approach, the size of $\tilde{\nu}$ in (2), is $\tilde{T} = \sum_{k=0}^{K-1} T_k$.

From our observations, the multi-ROM method increases this truncation order, i.e. $\tilde{T} \geq T$. It comes from a slower decrease of the singular value distribution of each submatrix $\mathbf{A}_k$ relatively to their maximum magnitude.

3) Conservation of the information: It is important to characterize the impact of the subdivision of Σ on the obtained basis in $\tilde{\mathbf{U}}$. If another SVD is applied to $\tilde{\mathbf{U}}\tilde{\mathbf{S}}$ where $\tilde{\mathbf{S}}$ contains the singular value distributions of each sub-ROM $\mathbf{U}_k$, we obtain the same distribution as if a single SVD was performed on $\mathbf{A}$, as it is shown in Section III. It indicates that the separation of Σ with this process does not deteriorate the amount of information contained in the original problem but now obtained through multiple ROMs instead of a single ROM, validating the approach from an information point of view. Furthermore, as shown in the validation cases, the accuracy of the characterization is preserved.

4) Reference point for multiple ROM: In the far field of the AUT, the reference point method enables to translate an electromagnetic source by applying a phase term to the radiated field [11]. Since the matrices A_k father the field radiated by the equivalent currents, our sources, these sources can be translated as well as the ROM basis in U_k in the same way. If the surface Σ is divided into identical regions Σ_k, which are a translation of a reference region Σ_{ref}, the following holds

$$\mathbf{U}_k = \mathbf{D}\mathbf{U}_{ref}, \tag{3}$$

where D is a diagonal matrix in which the i-th diagonal element is $d_i = \exp\left(jk\delta_k \cdot \frac{r_i}{|r_i|}\right)$. k is the wavenumber, r_i the i-th sampling position and δ_k is the translation vector transforming Σ_{ref} into Σ_k.

III. Application and Validation

A. Methodology

The multi-ROM approach is applied to simulated and measured data. These validations focus on several aspects to investigate the properties of the technique: the accuracy of the reconstruction of the far field, the variation of the total order of the model, $\tilde{T}$, the impact of equivalent currents and the application of the reference point method.

To evaluate the accuracy of the field reconstruction, a reference radiation pattern contained in the data vector $\mathbf{y}$ is compared against the reconstructed one, $\tilde{\mathbf{y}}$. The complex error is computed point-wise by the complex error signal defined as $\text{Error}(\mathbf{y}, \tilde{\mathbf{y}}) = \frac{|\mathbf{y}-\tilde{\mathbf{y}}|}{\|\mathbf{y}\|_\infty}$, where $\|\cdot\|_\infty$ is the maximum magnitude contained in $\mathbf{y}$. The Equivalent Noise Level (ENL) is defined to be the mean of that signal error. Both errors are given in dB.

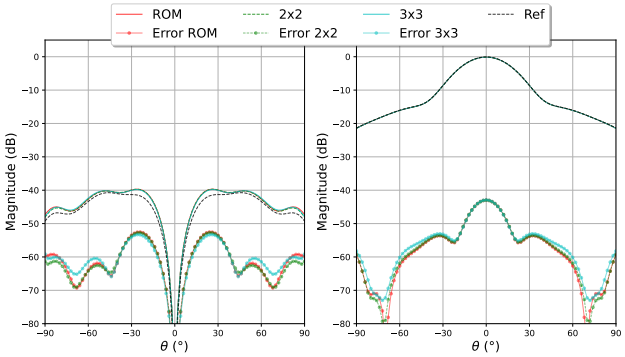

Fig. 1. Simulated E-plane horn: reconstruction of the far field for $\varphi = 45°$, (left) cross-polarization, and (right) co-polarization.

B. Simulation of a E-plane Horn

In this first application, the field comes from the simulation of a 3 GHz E-plane horn of dimensions $(2, 2, 3)\lambda$ ($\lambda = 0.1$ m), according to the Euclidian antenna's referential. The reduced sampling has only 664 points on the hemisphere while 1326 are required for a standard spherical measurement using spherical waves.

As Table I shows, the same error level is achieved for the three tested decompositions: the full surface Σ and two regular subdivisions of Σ in 2×2 and 3×3 regions. The far field is shown on the cutting plane $\varphi = 45°$ in Figure 1, further indicating that very similar reconstructions are achieved.

TABLE I
Reconstruction Accuracy of the Far Field of the Horn Antenna.

	full plan	2×2	3×3	3×3 w/ ref. point
ENL (dB)	-74.0	-76.4	-74.5	-75.3
$\tilde{T}$	176	311	374	374

Table I also clearly shows that $\tilde{T} \geq T$. The singular values distributions are presented in Figure 2. It illustrates the property evoked in the conservation of the information as the double SVD (SVD of the multi-ROM method) leads to the same information as the direct, complete, ROM.

The retrieved equivalent currents on Σ for a 3×3 decomposition where the multi-ROM method is obtained with or without transition currents between the domains are shown

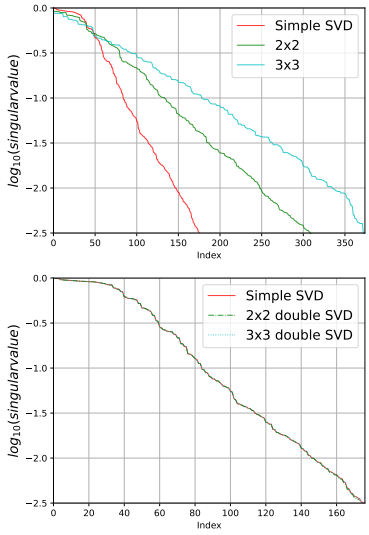

Fig. 2. Simulated E-plane horn: (top) distribution of normalized singular values for each set of decomposition, and (bottom) comparison between a single SVD on $\mathbf{A}$ and double SVD for 2×2 and 3×3 decomposition.

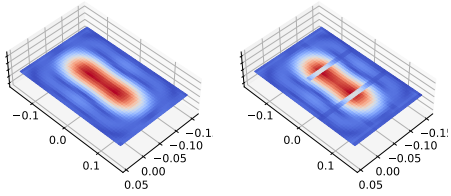

(a) (b)

Fig. 3. Simulated E-plane horn: modulus of the retrieved equivalent currents on Σ, (a) with interconnected domains and (b) without. In both cases, a multi-ROM has been applied.

in Figure 3. Simply putting disconnected current distributions next to each other is not enough to retrieve the expected, continuous, currents. However, with the proposed approach, the correct behavior is observed. Finally, the reference point method is used to to compute the multiple ROMs for a 3×3 decomposition. The middle square is used as our reference, providing $\mathbf{U}_{ref}$ in (3) to deduce the 8 other ones. As shown by the cutting planes of the field reconstruction in Figure 4, and by the ENL in Table I, the same reconstruction is achieved while only one SVD of a significantly smaller region is computed.

C. Patcharray

The second benchmark is a 3×3 array of rectangular E-plane patches at 10 GHz of dimensions $(3, 3, 1)\lambda$ ($\lambda = 0.03$ m). The reduced sampling has 656 points on the hemisphere while 1225 are required for a standard spherical measurement using spherical waves.

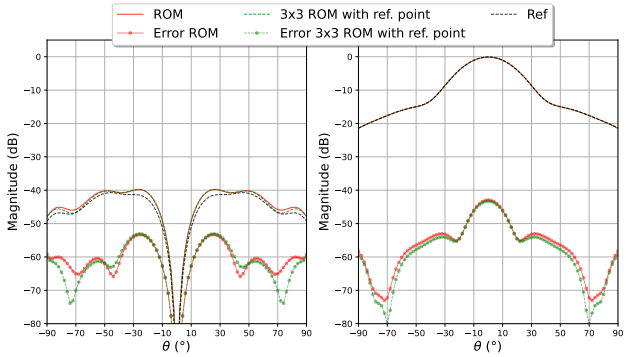

Fig. 4. Simulated E-plane horn: reconstruction of the far-field using the standard ROM approach or a 3×3 decomposition coupled with reference point method at $\varphi = 0°$.

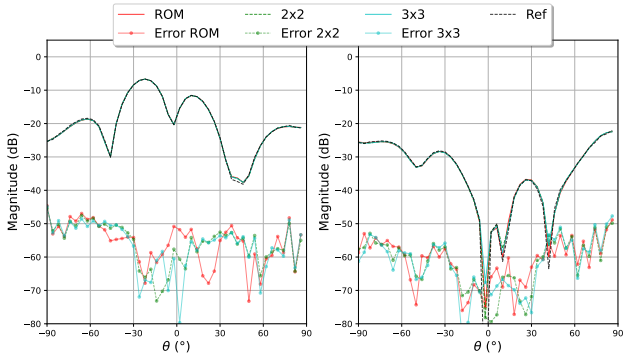

Fig. 5. Simulated patch array: Reconstruction of the field for $\varphi = 45°$.

The accuracy of far-field reconstructions are presented in Table II. They demonstrate the same behaviour as for the E-plane horn in terms of the total order $\tilde{T}$. In this case, a better accuracy is achieved for a finer subdivision of Σ. This can be explained by the introduction of more degrees of freedom relatively to the number of unknowns. The reconstructions of the field presented in Figure 5 show similar error signal levels for each subdivision of Σ.

The distributions of the singular values are also detailed in Table II and have the same shape as in Figure 2, where $\tilde{T}$ is larger for smaller decompositions of Σ. The information is still retained during the SVD process, with the singular values distributions for the SVD of the complete radiation matrix $\mathbf{A}$ and the double SVD for 2×2 and 3×3 decompositions.

Finally, the reference point approach is also used and the results are presented in Figure 6 and the ENL is reported in the Table II. The reconstruction is again as good as in the case of the multi-ROM approach with one SVD per subdomain.

TABLE II
RECONSTRUCTION ACCURACY OF THE FAR FIELD OF THE PATCHARRAY.

	full plan	2×2	3×3	3×3 w/ ref. point
ENL (dB)	-52.7	-60.8	-60.4	-60.3
$\tilde{T}$	197	351	498	498

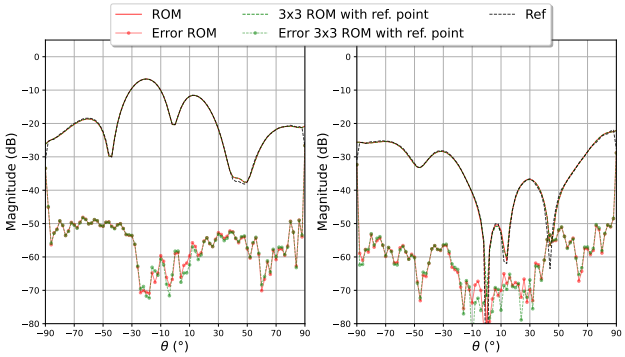

Fig. 6. Comparison between the classical ROM approach and a 3×3 decomposition with reference point at $\varphi = 45°$.

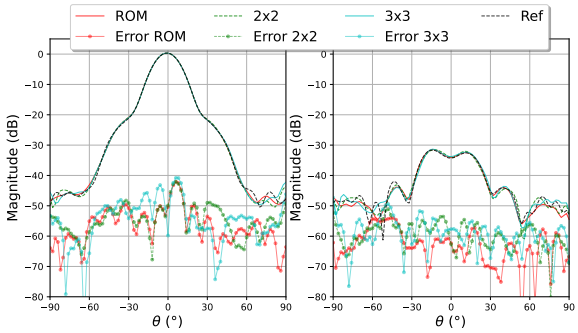

Fig. 7. Measured horn antenna: reconstruction of the field for $\varphi = 45°$.

D. Measured Horn

To conclude, a measured 26 GHz horn antenna of dimensions $(4, 4, 5)\lambda$ ($\lambda = 0.011$ m) is studied. The reduced sampling has 2550 points on the hemisphere while 2736 are required for a standard spherical measurement using spherical waves. As Table III shows, the same kind of difference between each truncation order as for the simulated cases is obtained. The main difference is in the accuracy of the far-field reconstruction, where the impact of the redundancies in the retained informations during the SVD process is more important in a measured case, hence a better ENL for the full plan domain, or for the reference point approach. As Figures 7 and 8 show, in every studied case, the multi-ROM approach, and in particular with the reference point method, leads to very good reconstructions.

TABLE III
RECONSTRUCTION OF THE FAR FIELD, MEASURED HORN ANTENNA.

	full plan	2×2	3×3	3×3 w/ ref. point
ENL (dB)	-53.2	-49.0	-47.4	-53.5
$\tilde{T}$	438	715	984	984

IV. Conclusion

The use of several ROMs on the same planar equivalent surface has been investigated. It has been shown that this approach does not deteriorate accuracy as compared to using a single ROM. Moreover, this approach offers some flexibility by adapting the order of each ROM to the complexity of equivalent currents, which may differ a lot depending on the region around the antenna under test.

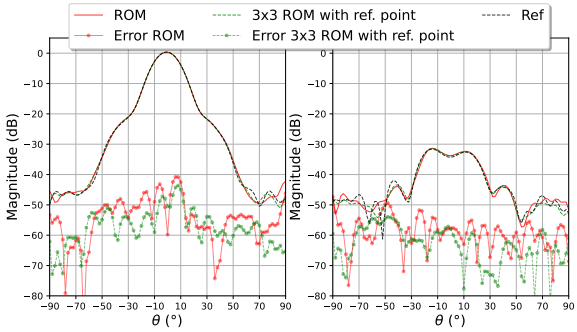

Fig. 8. Comparison between the classical ROM approach and a 3×3 decomposition with reference point at $\varphi = 45°$.

Acknowledgment

This publication is supported by the European Union through the European Regional Development Fund (ERDF), and by the Ministry of Higher Education and Research, Brittany, Rennes Métropole and Conseils Départementaux 35 and 22, through the CPER Projects SOPHIE / STIC & Ondes and CyMoCoD.

References

[1] J. Hald, J. Hansen, F. Jensen, and F. Larsen, *Spherical Near Field Antenna Measurements*. Peter Peregrinus, 1988.

[2] S. Gregson, J. McCormick, and C. Parini, *Principles of Planar Near-Field Antenna Measurements*. IET, 2007, vol. Series 53.

[3] D. Loschenbrand and C. Mecklenbräuker, "Fast antenna characterization via a sparse spherical multipole expansion." Aachen: 4th International Workshop on Compressed Sensing Theory and its Applications to Radar, Sonar and Remote, 2016.

[4] G. Giordanengo, M. Righero, F. Vipiana, M. Sabbadini, and G. Vecchi, "Fast antenna testing with reduced near field sampling," *IEEE Trans. on Antennas and Propag.*, vol. 62, no. 5, pp. 2501–2513, May 2014.

[5] B. Fuchs and A. Polimeridis, "Reduced-order models for fast antenna characterization," *IEEE Trans. on Antennas and Propag.*, vol. 67, no. 8, pp. 5673–5677, Aug. 2019.

[6] N. Mézières, M. Mattes, and B. Fuchs, "Antenna characterization from a small number of far-field measurements via reduced-order models," *IEEE Trans. on Antennas and Prop.*, 2021.

[7] O. M. Bucci, C. Gennarelli, and C. Savarese, "Representation of electromagnetic fields over arbitrary surfaces by a finite and nonredundant number of samples," *IEEE Trans. on Antennas and Propag.*, vol. 46, no. 3, pp. 351–359, March 1998.

[8] R. F. Harrington, *Time-Harmonic Electromagnetic Fields*. IEEE-Press, 2001. [Online]. Available: http://dx.doi.org/10.1109/9780470546710

[9] B. Fuchs, L. Le Coq, S. Rondineau, and M. D. Migliore, "Fast antenna far-field characterization via sparse spherical harmonic expansion," *IEEE Transactions on Antennas and Propagation*, vol. 65, no. 10, pp. 5503–5510, 2017.

[10] S. Corre, L. Le Coq, N. Mézières, M. Mattes, and B. Fuchs, "Numerical considerations to improve the reduced-order model approach for antenna measurements," in *2022 Antenna Measurement Techniques Association Symposium (AMTA)*, 2022, pp. 1–6.

[11] J.-p. Shang, D. min Fu, Y. bo Deng, and S. Jiang, "Measurement of phase center for antenna with the method of moving reference point," in *2008 8th International Symposium on Antennas, Propagation and EM Theory*, 2008, pp. 114–117.